CORA Cork Open Research Archive
Cartlann Taighde Oscailte Chorcaí

Title	Portable broadband cavity-enhanced spectrometer utilizing Kalman filtering: application to real-time, in situ monitoring of glyoxal and nitrogen dioxide
Authors	Fang, Bo;Zhao, Weixiong;Xu, Xuezhe;Zhou, Jiacheng;Ma, Xiao;Wang, Shuo;Zhang, Weijun;Venables, Dean S.;Chen, Weidong
Publication date	2017
Original Citation	Fang, B., Zhao, W., Xu, X., Zhou, J., Ma, X., Wang, S., Zhang, W., Venables, D. S. and Chen, W. (2017) 'Portable broadband cavity-enhanced spectrometer utilizing Kalman filtering: application to real-time, in situ monitoring of glyoxal and nitrogen dioxide', Optics Express, 25(22), pp. 26910-26922. doi: 10.1364/OE.25.026910
Type of publication	Article (peer-reviewed)
Link to publisher's version	https://www.osapublishing.org/oe/abstract.cfm?uri=oe-25-22-26910 - 10.1364/OE.25.026910
Rights	© 2017, Optical Society of America under the terms of the OSA Open Access Publishing Agreement
Download date	2026-11-15 01:09:41
Item downloaded from	https://hdl.handle.net/10468/6885



UCC
University College Cork, Ireland
Coláiste na hOllscoile Corcaigh

Research Article | Vol. 25, No. 22 | 30 Oct 2017 | OPTICS EXPRESS 26910
Optics EXPRESS

Portable broadband cavity-enhanced spectrometer utilizing Kalman filtering: application to real-time, *in situ* monitoring of glyoxal and nitrogen dioxide

Bo Fang,[1] Weixiong Zhao,[1,6] Xuezhe Xu,[1,2] Jiacheng Zhou,[1,2] Xiao Ma,[1,2] Shuo Wang,[1,2] Weijun Zhang,[1,2,3,7] Dean S. Venables,[4] and Weidong Chen[5]

[1]*Laboratory of Atmospheric Physico-Chemistry, Anhui Institute of Optics and Fine Mechanics, Chinese Academy of Sciences, Hefei, 230031, Anhui, China*
[2]*University of Science and Technology of China, Hefei, 230026, Anhui, China*
[3]*School of Environmental Science and Optoelectronic Technology, University of Science and Technology of China, Hefei, 230026, Anhui, China*
[4]*Department of Chemistry and Environmental Research Institute, University College Cork, Cork, Ireland*
[5]*Laboratoire de Physicochimie de l'Atmosphère, Université du Littoral Côte d'Opale, 59140 Dunkerque, France*
[6]*wxzhao@aiofm.ac.cn*
[7]*wjzhang@aiofm.ac.cn*

Abstract: This article describes the development and field application of a portable broadband cavity enhanced spectrometer (BBCES) operating in the spectral range of 440-480 nm for sensitive, real-time, *in situ* measurement of ambient glyoxal (CHOCHO) and nitrogen dioxide (NO_2). The instrument utilized a custom cage system in which the same SMA collimators were used in the transmitter and receiver units for coupling the LED light into the cavity and collecting the light transmitted through the cavity. This configuration realised a compact and stable optical system that could be easily aligned. The dimensions and mass of the optical layer were 676 × 74 × 86 mm^3 and 4.5 kg, respectively. The cavity base length was about 42 cm. The mirror reflectivity at λ = 460 nm was determined to be 0.9998, giving an effective absorption pathlength of 2.26 km. The demonstrated measurement precisions (1σ) over 60 s were 28 and 50 pptv for CHOCHO and NO_2 and the respective accuracies were 5% and 4%. By applying a Kalman adaptive filter to the retrieved concentrations, the measurement precisions of CHOCHO and NO_2 were improved to 8 pptv and 40 pptv in 21 s.

© 2017 Optical Society of America under the terms of the OSA Open Access Publishing Agreement

OCIS codes: (010.1120) Air pollution monitoring; (120.4640) Optical instruments; (300.6550) Spectroscopy, visible.

References and links

1. A. J. Huisman, J. R. Hottle, M. M. Galloway, J. P. DiGangi, K. L. Coens, W. Choi, I. C. Faloona, J. B. Gilman, W. C. Kuster, J. de Gouw, N. C. Bouvier-Brown, A. H. Goldstein, B. W. LaFranchi, R. C. Cohen, G. M. Wolfe, J. A. Thornton, K. S. Docherty, D. K. Farmer, M. J. Cubison, J. L. Jimenez, J. Mao, W. H. Brune, and F. N. Keutsch, "Photochemical modeling of glyoxal at a rural site: observations and analysis from BEARPEX 2007," Atmos. Chem. Phys. **11**(17), 8883–8897 (2011).
2. T. M. Fu, D. J. Jacob, F. Wittrock, J. P. Burrows, M. Vrekoussis, and D. K. Henze, "Global budgets of atmospheric glyoxal and methylglyoxal, and implications for formation of secondary organic aerosols," J. Geophys. Res. **113**(D15), D15303 (2008).
3. R. Volkamer, F. San Martini, L. T. Molina, D. Salcedo, J. L. Jimenez, and M. J. Molina, "A missing sink for gas-phase glyoxal in Mexico City: Formation of secondary organic aerosol," Geophys. Res. Lett. **34**(19), L19807 (2007).
4. X. Pang, A. C. Lewis, A. R. Rickard, M. T. Baeza-Romero, T. J. Adams, S. M. Ball, M. J. S. Daniels, I. C. A. Goodall, P. S. Monks, S. Peppe, M. Ródenas García, P. Sánchez, and A. Muñoz, "A smog chamber comparison

#307846 https://doi.org/10.1364/OE.25.026910
Journal © 2017 Received 25 Sep 2017; revised 15 Oct 2017; accepted 17 Oct 2017; published 19 Oct 2017

Optics EXPRESS

of a microfluidic derivatisation measurement of gas-phase glyoxal and methylglyoxal with other analytical techniques," Atmos. Meas. Tech. **7**(2), 373–389 (2014).
5. R. Thalman, M. T. Baeza-Romero, S. M. Ball, E. Borrás, M. J. S. Daniels, I. C. A. Goodall, S. B. Henry, T. Karl, F. N. Keutsch, S. Kim, J. Mak, P. S. Monks, A. Muñoz, J. Orlando, S. Peppe, A. R. Rickard, M. Ródenas, P. Sánchez, R. Seco, L. Su, G. Tyndall, M. Vázquez, T. Vera, E. Waxman, and R. Volkamer, "Instrument intercomparison of glyoxal, methyl glyoxal and NO_2 under simulated atmospheric conditions," Atmos. Meas. Tech. **8**(4), 1835–1862 (2015).
6. S. B. Henry, A. Kammrath, and F. N. Keutsch, "Quantification of gas-phase glyoxal and methylglyoxal via the Laser-Induced Phosphorescence of (methyl) GLyOxal Spectrometry (LIPGLOS) Method," Atmos. Meas. Tech. **5**(1), 181–192 (2012).
7. U. Platt and J. Stutz, *Differential Optical Absorption Spectroscopy. Principles and Applications* (Springer-Verlag Berlin Heidelberg, 2008).
8. R. Volkamer, L. T. Molina, M. J. Molina, T. Shirley, and W. H. Brune, "DOAS measurement of glyoxal as an indicator for fast VOC chemistry in urban air," Geophys. Res. Lett. **32**(8), L08806 (2005).
9. R. Sinreich, R. Volkamer, F. Filsinger, U. Frieß, C. Kern, U. Platt, O. Sebastián, and T. Wagner, "MAX-DOAS detection of glyoxal during ICARTT 2004," Atmos. Chem. Phys. **7**(5), 1293–1303 (2007).
10. F. Peng, T. Luo, Y. Yuang, L. Qiu, P. Xie, and W. Liu, "Elimination of atmospheric interfering absorption for the measurement of glyoxal by LP-DOAS," Guangzi Xuebao **39**(10), 1889–1895 (2010).
11. S. Baidar, H. Oetjen, S. Coburn, B. Dix, I. Ortega, R. Sinreich, and R. Volkamer, "The CU Airborne MAX-DOAS instrument: vertical profiling of aerosol extinction and trace gases," Atmos. Meas. Tech. **6**(3), 719–739 (2013).
12. X. Li, T. Brauers, A. Hofzumahaus, K. Lu, Y. P. Li, M. Shao, T. Wagner, and A. Wahner, "MAX-DOAS measurements of NO_2, HCHO and CHOCHO at a rural site in Southern China," Atmos. Chem. Phys. **13**(4), 2133–2151 (2013).
13. Z. Liu, Y. Wang, M. Vrekoussis, A. Richter, F. Wittrock, J. P. Burrows, M. Shao, C. C. Chang, S. C. Liu, H. Wang, and C. Cheng, "Exploring the missing source of glyoxal (CHOCHO) over China," Geophys. Res. Lett. **39**(10), L10812 (2012).
14. F. Wittrock, A. Richter, H. Oetjen, J. P. Burrows, M. Kanakidou, S. Myriokefalitakis, R. Volkamer, S. Beirle, U. Platt, and T. Wagner, "Simultaneous global observations of glyoxal and formaldehyde from space," Geophys. Res. Lett. **33**(16), L16804 (2006).
15. C. Chan Miller, G. Gonzalez Abad, H. Wang, X. Liu, T. Kurosu, D. J. Jacob, and K. Chance, "Glyoxal retrieval from the Ozone Monitoring Instrument," Atmos. Meas. Tech. **7**(11), 3891–3907 (2014).
16. S. Ball and R. Jones, "Broadband Cavity Ring-Down Spectroscopy," in *Cavity Ring-Down Spectroscopy: Techniques and Applications*, G. Berden and R. Engeln, eds. (John Wiley & Sons, Ltd, 2009).
17. A. A. Ruth, S. Dixneuf, and R. Raghunandan, "Broadband Cavity-Enhanced Absorption Spectroscopy with Incoherent Light," in *Cavity-Enhanced Spectroscopy and Sensing*, G. Gagliardi and H. P. Loock, eds. (Springer-Verlag Berlin Heidelberg, 2014).
18. R. A. Washenfelder, A. O. Langford, H. Fuchs, and S. S. Brown, "Measurement of glyoxal using an incoherent broadband cavity enhanced absorption spectrometer," Atmos. Chem. Phys. **8**(24), 7779–7793 (2008).
19. R. Thalman and R. Volkamer, "Inherent calibration of a blue LED-CE-DOAS instrument to measure iodine oxide, glyoxal, methyl glyoxal, nitrogen dioxide, water vapour and aerosol extinction in open cavity mode," Atmos. Meas. Tech. **3**(6), 1797–1814 (2010).
20. S. Coburn, I. Ortega, R. Thalman, B. Blomquist, C. W. Fairall, and R. Volkamer, "Measurements of diurnal variations and eddy covariance (EC) fluxes of glyoxal in the tropical marine boundary layer: description of the Fast LED-CE-DOAS instrument," Atmos. Meas. Tech. **7**(10), 3579–3595 (2014).
21. R. Volkamer, S. Baidar, T. L. Campos, S. Coburn, J. P. DiGangi, B. Dix, E. W. Eloranta, T. K. Koenig, B. Morley, I. Ortega, B. R. Pierce, M. Reeves, R. Sinreich, S. Wang, M. A. Zondlo, and P. A. Romashkin, "Aircraft measurements of BrO, IO, glyoxal, NO_2, H_2O, O_2–O_2 and aerosol extinction profiles in the tropics: comparison with aircraft-/ship-based in situ and lidar measurements," Atmos. Meas. Tech. **8**(5), 2121–2148 (2015).
22. K. E. Min, R. A. Washenfelder, W. P. Dubé, A. O. Langford, P. M. Edwards, K. J. Zarzana, J. Stutz, K. Lu, F. Rohrer, Y. Zhang, and S. S. Brown, "A broadband cavity enhanced absorption spectrometer for aircraft measurements of glyoxal, methylglyoxal, nitrous acid, nitrogen dioxide, and water vapor," Atmos. Meas. Tech. **9**(2), 423–440 (2016).
23. S. E. Fiedler, A. Hese, and A. A. Ruth, "Incoherent broad-band cavity-enhanced absorption spectroscopy," Chem. Phys. Lett. **371**(3–4), 284–294 (2003).
24. W. Zhao, M. Dong, W. Chen, X. Gu, C. Hu, X. Gao, W. Huang, and W. Zhang, "Wavelength-resolved optical extinction measurements of aerosols using broad-band cavity-enhanced absorption spectroscopy over the spectral range of 445-480 nm," Anal. Chem. **85**(4), 2260–2268 (2013).
25. H. Yi, T. Wu, G. Wang, W. Zhao, E. Fertein, C. Coeur, X. Gao, W. Zhang, and W. Chen, "Sensing atmospheric reactive species using light emitting diode by incoherent broadband cavity enhanced absorption spectroscopy," Opt. Express **24**(10), A781–A790 (2016).
26. W. Zhao, X. Xu, B. Fang, Q. Zhang, X. Qian, S. Wang, P. Liu, W. Zhang, Z. Wang, D. Liu, Y. Huang, D. S. Venables, and W. Chen, "Development of an incoherent broad-band cavity-enhanced aerosol extinction spectrometer and its application to measurement of aerosol optical hygroscopicity," Appl. Opt. **56**(11), E16–E22 (2017).

Optics EXPRESS

27. Y. Chen, C. Yang, W. Zhao, B. Fang, X. Xu, Y. Gai, X. Lin, W. Chen, and W. Zhang, "Ultra-sensitive measurement of peroxy radicals by chemical amplification broadband cavity-enhanced spectroscopy," Analyst (Lond.) **141**(20), 5870–5878 (2016).
28. W. Zhao, X. Xu, M. Dong, W. Chen, X. Gu, C. Hu, Y. Huang, X. Gao, W. Huang, and W. Zhang, "Development of a cavity-enhanced aerosol albedometer," Atmos. Meas. Tech. **7**(8), 2551–2566 (2014).
29. P. Werle, R. Mücke, and F. Slemr, "The limits of signal averaging in atmospheric trace-gas monitoring by tunable diode-laser absorption spectroscopy (TDLAS)," Appl. Phys. B **57**(2), 131–139 (1993).
30. R. E. Kalman, "A new approach to linear filtering and predication problems," Trans. ASME, J. Basic Eng. **82**(D), 35–45 (1960).
31. W. Chen, H. Yi, T. Wu, W. Zhao, C. Lengignon, G. Wang, E. Fertein, C. Coeur, G. Wysocki, T. Wang, M. W. Sigrist, X. Gao, and W. Zhang, "Photonic sensing of reactive atmospheric species," Encyclopedia of Analytical Chemistry, 1–60 (2017).
32. D. P. Leleux, R. Claps, W. Chen, F. K. Tittel, and T. L. Harman, "Applications of Kalman filtering to real-time trace gas concentration measurements," Appl. Phys. B **74**(1), 85–93 (2002).
33. P. W. Werle, B. Scheumann, and J. Schandl, "Real-time signal-processing concepts for trace-gas analysis by diode-laser spectroscopy," Opt. Eng. **33**(9), 3093–3105 (1994).
34. H. Riris, C. B. Carlisle, and R. E. Warren, "Kalman filtering of tunable diode laser spectrometer absorbance measurements," Appl. Opt. **33**(24), 5506–5508 (1994).
35. T. Wu, W. Chen, E. Kerstel, E. Fertein, X. Gao, J. Koeth, K. Rössner, and D. Brückner, "Kalman filtering real-time measurements of H_2O isotopologue ratios by laser absorption spectroscopy at 2.73 μm," Opt. Lett. **35**(5), 634–636 (2010).
36. T. Wu, W. Chen, E. Fertein, P. Masselin, X. Gao, W. Zhang, Y. Wang, J. Koeth, D. Brückner, and X. He, "Measurement of the D/H, $^{18}O/^{16}O$, and $^{17}O/^{16}O$ isotope ratios in water by laser absorption spectroscopy at 2.73 μm," Sensors (Basel) **14**(5), 9027–9045 (2014).
37. T. Wu, W. Zhao, W. Chen, and X. Gao, "Incoherent broadband cavity enhanced absorption spectroscopy for in situ measurements of NO_2 with a blue light emitting diode," Appl. Phys. B **94**(1), 85–94 (2009).
38. S. Vaughan, T. Gherman, A. A. Ruth, and J. Orphal, "Incoherent broad-band cavity-enhanced absorption spectroscopy of the marine boundary layer species I_2, IO and OIO," Phys. Chem. Chem. Phys. **10**(30), 4471–4477 (2008).
39. R. Thalman, K. J. Zarzana, M. A. Tolbert, and R. Volkamer, "Rayleigh scattering cross-section measurements of nitrogen, argon, oxygen and air," J. Quant. Spectrosc. Radiat. Transf. **147**(5), 171–177 (2014).
40. H. Naus and W. Ubachs, "Experimental verification of Rayleigh scattering cross sections," Opt. Lett. **25**(5), 347–349 (2000).
41. M. Sneep and W. Ubachs, "Direct measurement of the Rayleigh scattering cross section in various gases," J. Quant. Spectrosc. Radiat. Transf. **92**(3), 293–310 (2005).
42. R. Volkamer, P. Spietz, J. P. Burrows, and U. Platt, "High-resolution absorption cross-sections of glyoxal in the UV-vis and IR spectral ranges," J. Photochem. Photobiol. Chem. **172**(1), 35–46 (2005).
43. A. C. Vandaele, C. Hermans, S. Fally, M. Carleer, R. Colin, M. F. Mérienne, and A. Jenouvrier, "High-resolution Fourier transform measurement of the NO_2 visible and near-infrared absorption cross-section: Temperature and pressure effects," J. Geophys. Res. **107**(D18), 4348 (2002).
44. R. Thalman and R. Volkamer, "Temperature dependent absorption cross-sections of O_2-O_2 collision pairs between 340 and 630 nm and at atmospherically relevant pressure," Phys. Chem. Chem. Phys. **15**(37), 15371–15381 (2013).
45. R. Meller, W. Raber, J. N. Crowley, M. E. Jenkin, and G. K. Moortgat, "The UV-visible absorption spectrum of methylglyoxal," J. Photochem. Photobiol. Chem. **62**(2), 163–171 (1991).
46. H. Keller-Rudek, G. K. Moortgat, R. Sander, and R. Sörensen, "The MPI-Mainz UV/VIS spectral atlas of gaseous molecules of atmospheric interest," Earth Syst. Sci. Data **5**(2), 365–373 (2013).
47. C. S. Goldenstein, V. A. Millera, R. M. Spearrina, and C. L. Stranda, "SpectraPlot.com: Integrated spectroscopic modeling of atomic and molecular gases," J. Quant. Spectrosc. Radiat. Transf. **200**, 249–257 (2017).
48. L. S. Rothman, I. E. Gordon, Y. Babikov, A. Barbe, D. Chris Benner, P. F. Bernath, M. Birk, L. Bizzocchi, V. Boudon, L. R. Brown, A. Campargue, K. Chance, E. A. Cohen, L. H. Coudert, V. M. Devi, B. J. Drouin, A. Fayt, J. M. Flaud, R. R. Gamache, J. J. Harrison, J. M. Hartmann, C. Hill, J. Hodges, D. Jacquemart, A. Jolly, J. Lamouroux, R. J. Le Roy, G. Li, D. A. Long, O. M. Lyulin, C. J. Mackie, S. T. Massie, S. N. Mikhailenko, H. S. P. Muller, O. V. Naumenko, A. V. Nikitin, J. Orphal, V. I. Perevalov, A. Perrin, E. R. Polovtseva, C. Richard, M. A. H. Smith, E. Starikova, K. Sung, S. Tashkun, J. Tennyson, G. C. Toon, V. G. Tyuterev, and G. Wagner, "The HITRAN2012 molecular spectroscopic database," J. Quant. Spectrosc. Radiat. Transf. **130**, 4–50 (2013).
49. J. M. Langridge, S. M. Ball, and R. L. Jones, "A compact broadband cavity enhanced absorption spectrometer for detection of atmospheric NO_2 using light emitting diodes," Analyst (Lond.) **131**(8), 916–922 (2006).
50. O. J. Kennedy, B. Ouyang, J. M. Langridge, M. J. S. Daniels, S. Bauguitte, R. Freshwater, M. W. McLeod, C. Ironmonger, J. Sendall, O. Norris, R. Nightingale, S. M. Ball, and R. L. Jones, "An aircraft based three channel broadband cavity enhanced absorption spectrometer for simultaneous measurements of NO_3, N_2O_5 and NO_2," Atmos. Meas. Tech. **4**(9), 1759–1776 (2011).
51. B. Ouyang and R. L. Jones, "Understanding the sensitivity of cavity-enhanced absorption spectroscopy: pathlength enhancement versus noise suppression," Appl. Phys. B **109**(4), 581–591 (2012).

Optics EXPRESS

52. T. Wu, W. Chen, E. Fertein, F. Cazier, D. Dewaele, and X. Gao, "Development of an open-path incoherent broadband cavity-enhanced spectroscopy based instrument for simultaneous measurement of HONO and NO_2 in ambient air," Appl. Phys. B **106**(2), 501–509 (2012).
53. T. D. Gordon, N. L. Wagner, M. S. Richardson, D. C. Law, D. Wolfe, E. W. Eloranta, C. A. Brock, F. Erdesz, and D. M. Murphy, "Design of a novel open-path aerosol extinction cavity ringdown spectrometer," Aerosol Sci. Technol. **49**(9), 717–726 (2015).

1. Introduction

Glyoxal (GLY, CHOCHO) is the smallest (α-)dicarbonyl and is present in the atmosphere as a first generation product from the photochemical oxidation of anthropogenic and biogenic volatile organic compounds (VOCs). It contributes significantly to the formation of secondary organic aerosol (SOA) and ozone (O_3) [1–3]. Its lifetime of a few hours makes it a promising indicator molecule for VOC oxidation chemistry on local and global scales [3].

Field measurements of CHOCHO are important because comparing observations to model predictions is a key test of our understanding of VOC photochemistry. Several approaches have been used to measure CHOCHO. These include chromatographic methods, like Gas Chromatography combined with a Flame Ionization Detector (GC-FID) [4], and spectroscopic methods such as Fourier Transform Infrared Spectrometer (FT-IR) [5], Laser-Induced Phosphorescence (LIP) [6], Differential Optical Absorption Spectroscopy (DOAS) [7–15], and Broadband Cavity-Enhanced Spectroscopy (BBCES) [16–22]. Details of intercomparisons of CHOCHO measurements are given in Refs [4] and [5].

Both DOAS and BBCES detect CHOCHO directly by measuring its unique and structured absorption in the visible spectral range (420 – 465 nm, with a maximum absorption peak at 455 nm). The first direct measurement of CHOCHO in the atmosphere by DOAS was demonstrated by Volkamer et al. in Mexico City in 2003 [8], where a detection precision of 150 pptv (parts per trillion by volume, 3σ) was achieved using a total absorption pathlength of 4420 m with 2 to 15 min integration times. In 2008, Washenfelder demonstrated a laboratory BBCES system that had a CHOCHO detection precision of 29 pptv (1σ) over 1 min sampling time [18]. The effective absorption pathlength was 17.9 km. Thalman and Volkamer [19] improved the detection sensitivity to a precision of 10 pptv (1σ) in 1 min with an effective pathlength of 13 km in 2010. Since then, other BBCES measurements of CHOCHO have been demonstrated on different platforms, including aircraft- and ship- based platforms [20–22].

Broadband cavity-enhanced techniques [16,17,23] use a relatively inexpensive incoherent broadband light, such as a Xenon arc lamp or a light emitting diode (LED), as the probe light for spectroscopic detection of trace gas. The light from the source is injected into a high finesse cavity formed by high reflectivity mirrors, and light transmitted through the cavity is dispersed and measured by a multichannel detector like a CCD spectrometer. Spectral fitting across a suitable window allows multiple species to be simultaneously quantified with good temporal resolution and high selectivity [18,19,24]. Compared to DOAS, which has a very long physical pathlength through the atmosphere, BBCES achieves comparable or superior sensitivity in a compact and robust system that is suited to mobile, high spatial resolution observations [17]. BBCES is also widely used for the measurement of other trace gases and atmospheric aerosol extinction [25–28], and references therein].

This article describes a BBCES instrument designed and constructed for sensitive detection of CHOCHO and NO_2 in China's Pearl River Delta (PRD) and Yangtze River Delta (YRD) regions. These measurements are needed to investigate VOC degradation mechanisms and their impact on air quality through the production of O_3 and fine particles. While similar in some respects to our previously described BBCES instruments [24,26,27], the new BBCES instrument has been significantly improved by using a custom cage system and symmetrical transmitter and receiver units. These changes have improved both the instrument's physical specifications (reduced size and mass) and its performance characteristics (superior sensitivity and stability).

Optics EXPRESS

Signal averaging can improve the detection precision up to an optimum averaging time (as defined in Allan variance analysis [29]) but is ultimately limited by electrical and optical noise and short-term gas concentration variations. The Kalman filtering algorithm, developed by Kalman in 1960 [30], is one of the successful post-processing techniques that allows efficient on-line filtering of concentration measurements [31,32]. This technique was first applied in tunable diode laser absorption spectroscopy (TDLAS) by Werle et al. [33]; it has since been extended to TDLAS based gas sensors [32,34] and real-time measurement of water isotopic ratios [35,36]. The Kalman filtering is computationally efficient, adaptive, and can adjust to changes in dynamic range during measurement without slowing the temporal response of the system [31,32]. This work presents the first time (to our knowledge) that Kalman filtering was applied in BBCES, for real-time optimization of the detection sensitivity and precision.

2. Experimental section

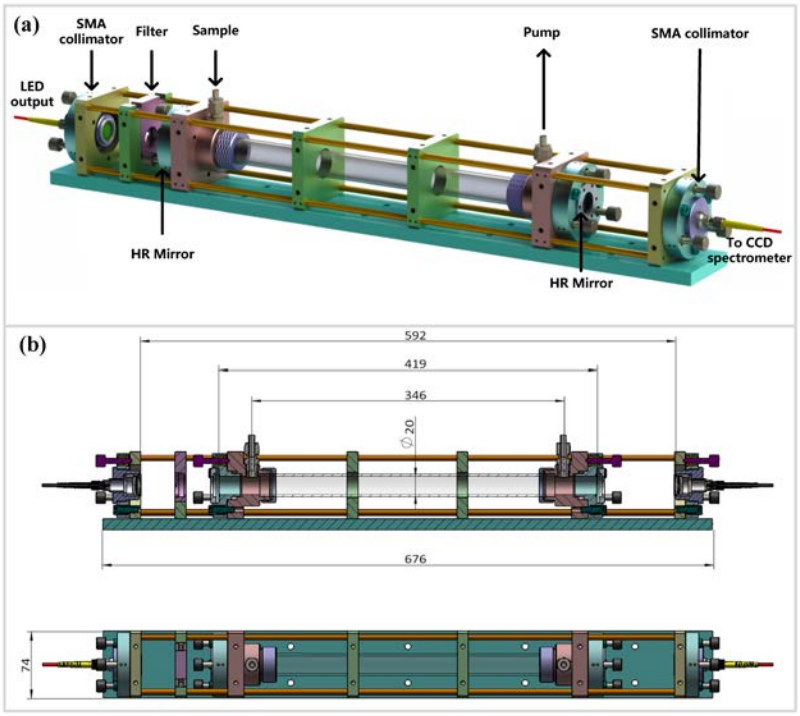


Fig. 1. (a) Layout of the custom cage based optical system. The coupling system for transmitter (LED output) and receiver units (CCD spectrometer) were interchangeable. (b) Side view of the optical system with dimensions in mm.

Figure 1 shows the optical layout of the BBCES instrument. The design is based around a custom cage system with dimensions of 676 × 74 × 86 mm^3. This optical subsystem had a mass of 4.5 kg. The output from a 5 W blue LED (LedEngin LZ110B200, mounted on a Peltier heat sink and controlled with chassis mount temperature and laser diode drivers from Wavelength Electronics) was coupled directly into a 500 μm core diameter multimode fiber (numerical aperture, NA = 0.22). It was then collimated with an SMA air-spaced doublet collimator (f = 34.74 mm, NA = 0.26) and injected into a high finesse optical cavity. The transmitted light was collected with an identical SMA air-spaced doublet collimator and fed via an identical multimode fiber into a CCD spectrometer (Ocean Optics Maya 2000 Pro) with a 200 μm width slit and a spectral resolution of about 0.35 nm. The CCD spectrometer and BBCES instrument were operated at room temperature. The total acquisition time of each

Optics EXPRESS

spectrum was equal to two times of the product of integration time of the CCD spectrometer and the number of scans to average, and an additional 1 s required for data processing. The duty cycle of the instrument was limited by the CCD control program, but can in principle be further improved by a factor of two.

The couplings for the transmitter and receiver units were symmetric and interchangeable. These SMA style connectors improved the compactness and stability of the optical system and the overall configuration simplifies optical alignment. Figure 2 shows the intensity spectrum transmitted through the cavity with an integration time of 20 ms, which covered the spectral region from 435 to 490 nm.

The optical cavity was made of an FEP tube with an inner diameter of 2 cm. The distance between the two highly reflective cavity mirrors (Layertec, 25 mm diameter) was about 42 cm, and the distance from the sample inlet to the outlet was about 35 cm. A Teflon particle filter (Parker, Balston) was placed at the sample inlet. Min et al. have reported that losses of CHOCHO and NO_2 on Teflon are negligible [22]. Since the sample gas stream was particle-free, no purge gas was used to protect cavity mirrors from particle deposition. The sample flow rate was 1.5 L/min and the residence time in the cavity was ~5 s.

3. Results and discussion

3.1 Data retrieval processing

In BBCES, the absorption coefficient α(λ) of the sample inside the cavity can be expressed as [23,24,37,38]:

$$\alpha(\lambda)=\frac{1}{d}\left(\frac{I_0(\lambda)}{I(\lambda)}-1\right)\left(1-R(\lambda)\right)=\sum_i n_i\sigma_i(s_i+t_i\lambda)+P(\lambda) \tag{1}$$

where d is the sample length, $R(\lambda)$ is the mirror reflectivity, and $I_0(\lambda)$ and $I(\lambda)$ are respectively the light intensities transmitted through the cavity when filled with clean reference air and when filled with the sample gas. n_i and σ_i are the number density and reference absorption cross section of the ith absorber, respectively. s_i and t_i are the shift and stretch coefficients for each absorber and are used to correct the wavelength calibration [24]. $P(\lambda)$, typically a 3rd order polynomial, was used to account for the background shape of the lamp emission spectrum.

The mirror reflectivity $R(\lambda)$ was determined from the Rayleigh scattering of N_2 and CO_2 using the following equation [18,26]:

$$R(\lambda)=1-d\left(\frac{\left(I_{CO_2}(\lambda)/I_{N_2}(\lambda)\right)\sigma_{Ray}^{CO_2}(\lambda)-\sigma_{Ray}^{N_2}(\lambda)}{1-I_{CO_2}(\lambda)/I_{N_2}(\lambda)}\right) \tag{2}$$

where $I_{CO2}(\lambda)$ and $I_{N2}(\lambda)$ are the light intensities transmitted through the cavity filled with either pure CO_2 or pure N_2, respectively. $\sigma_{Ray}^{CO_2}(\lambda)$ and $\sigma_{Ray}^{N_2}(\lambda)$ are the reference Rayleigh absorption cross sections of CO_2 and N_2 and have reported uncertainties of 4% and 1% [39–41]. Ten different pairs of CO_2 and N_2 transmissions were used to determine $R(\lambda)$. The standard deviation in measured (1 - R) was about 1% and the mean reflectivity value was used in Eq. (1). In this work, the $R(\lambda)$ at 460 nm was determined to be 99.98%, which implies an effective optical pathlength (L_{eff}) of about 2.26 km in the cavity.

Optics EXPRESS

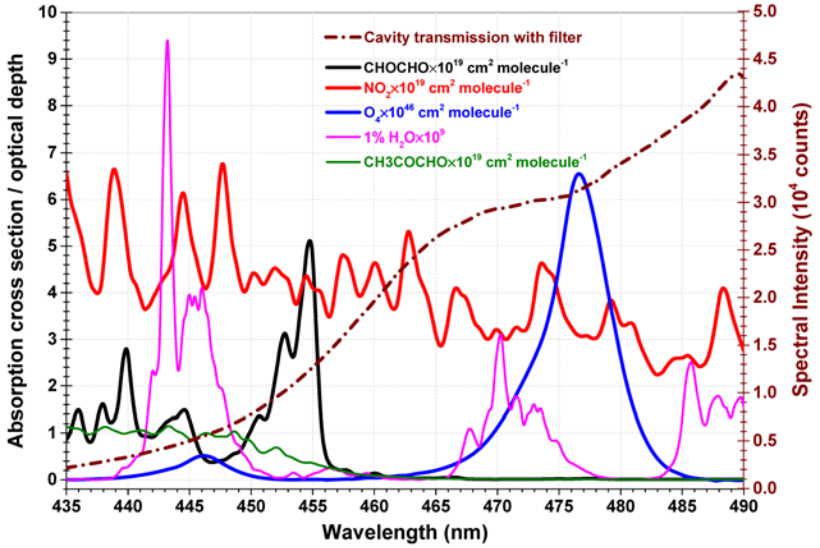


Fig. 2. Plot of the cavity transmission spectrum, convolved reference cross sections of CHOCHO, NO_2, O_4 and $CH_3COOCHO$, and absorption optical depth of 1% H_2O with 1 cm absorption pathlength at atmospheric pressure.

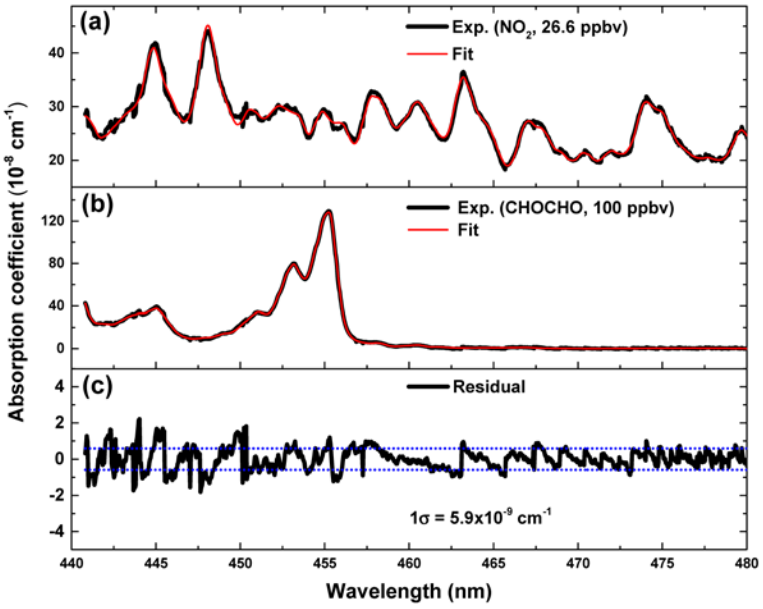


Fig. 3. Experimental absorption spectra of (a) NO_2 and (b) CHOCHO measured by BBCES associated with the fit residual (c). Red lines in (a) and (b) are the fitted absorption spectra for 26.6 ppbv NO_2 and 100 ppbv CHOCHO. The 1σ standard deviation of the fit residual was 5.9 × 10^{-9} cm^{-1} (denoted by the dotted lines in (c)) for a 3 s spectrum acquisition time.

The reference cross sections (σ) were generated by convoluting high-resolution literature absorption cross sections with a Gaussian line shape (FWHM = 0.68 nm) to represent the instrument function of the CCD spectrometer. The reference cross sections used for the spectral retrievals lie in the spectral range of 435 – 490 nm and are shown in Fig. 2. The high-resolution cross sections were those of Volkamer et al. [42] for CHOCHO (spectral resolution of 0.001 nm, 296 K), Vandaele et al. [43] for NO_2 (resolution of 0.1 cm^{-1}, 294 K), Thalman et

Optics EXPRESS

al. [44] for the O_2-O_2 collision pairs (O_4) at 293 K, and Meller et al. [45] for methylglyoxal ($CH_3COOCHO$) with a resolution of 0.07 nm at 296 K. These data can be accessed from the MPI-Mainz UV/VIS spectral atlas database [46]. The high-resolution H_2O absorption was calculated with the SpectraPlot program [47] based on the HITRAN2012 database at atmospheric pressure (with a mixing ratio of 1% and a 1 cm absorption path) [48]. The convolved optical depth of H_2O absorption is shown in Fig. 2.

As a demonstration of the simultaneous measurement of CHOCHO and NO_2, a mixture of these two species was introduced to the instrument. A representative measured spectrum and fitted spectrum between 440 nm and 480 nm is shown in Fig. 3. The total acquisition time for each spectrum was 3 s (20 ms integration time and 50 spectra averaging, with 1 s additional compensation time for data processing). The detection sensitivity was estimated to be 5.9×10^{-9} cm^{-1} based on the 1σ standard deviation of the spectral fit residual.

3.2 Precision, accuracy and detection limit

The accuracy of a measurement system reflects the closeness of a measured value to a true value, while the precision describes the degree to which repeated measurements under unchanged conditions show the same results (sometimes referred to as reproducibility or repeatability) [31]. In this work, the stability and precision of the BBCES instrument for CHOCHO and NO_2 were investigated using an Allan variance analysis. The upper panel of Fig. 4 shows a one hour time series measurement of particle-free zero air with a time resolution of 3 s. The Allan variance analysis is shown in the middle panel of Fig. 4. For NO_2 measurements, the measurement precision can be further improved to 0.02 ppbv with an averaging time of 192 s. For a 60 s integration time, the precision for NO_2 was 0.05 ppbv. For measurements of CHOCHO, the minimum (0.012 ppbv) in the Allan plot indicates that the optimum averaging time was 324 s. For a 60 s integration time, the precision for CHOCHO was about 0.028 ppbv.

The frequency distribution of the time series measurement of NO_2 and CHOCHO is shown in the lower panel of Fig. 4. A Gaussian distribution was fitted to the histograms to obtain the mean (the absolute offset from the zero reference spectrum, treated as "background" [5]) and standard deviation ($\sigma_{Gaussian}$, a measure of the actual instrument precision) of the zero air measurement. The mean and 1σ standard deviation values for NO_2 and CHOCHO were 0.018 and 0.181 ppbv, and 0.014 and 0.097 ppbv, respectively. A widely used 3σ Limit of Detection ($LOD_{expected,3\sigma}$) in analytical chemistry can be calculated from the histograms results [5]:

$$LOD_{expected,3\sigma} = 3 \cdot \sigma_{Gaussian} + |background| \quad (3)$$

For NO_2 and CHOCHO with 3 s total acquisition time, the expected LODs (3σ) were 0.561 ppbv and 0.305 ppbv, respectively, which agreed well with the instrument precisions (0.567 and 0.294 ppbv) based on 3σ standard deviations of the continuous measurement (upper panel of Fig. 4).

Optics EXPRESS

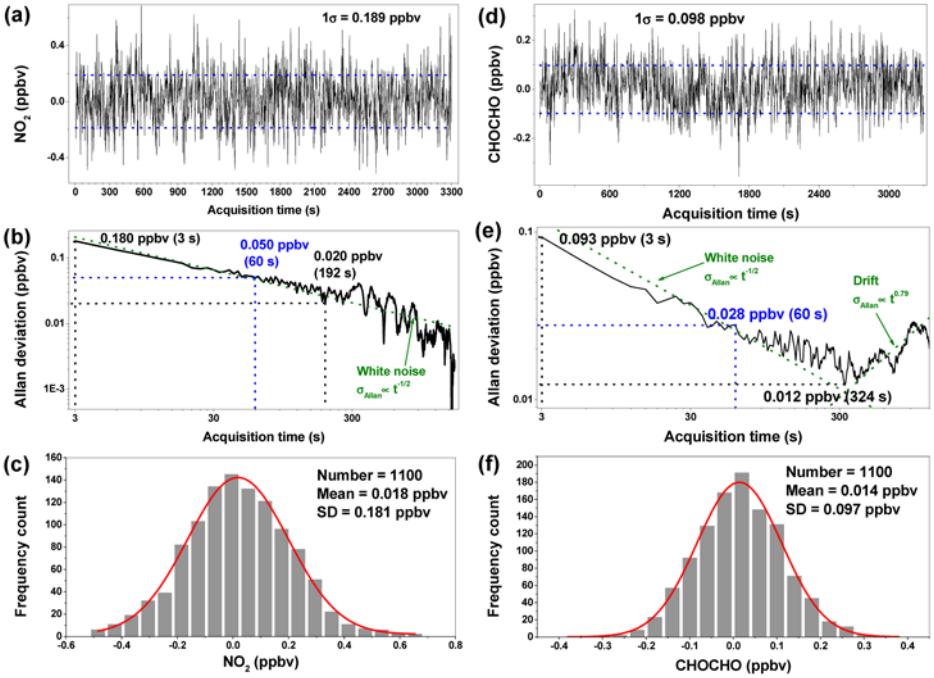


Fig. 4. Performance evaluation of the BBCES instrument for NO_2 (a-c) and CHOCHO (d-f) measurement with zero air. Upper panel: mixing ratio time series of NO_2 (a) and CHOCHO (d); middle panel: Allan deviation plots for NO_2 (b) and CHOCHO (e) mixing ratios. The white noise ($\sigma_{Allan} \propto t^{-1/2}$) and drift ($\sigma_{Allan} \propto t^{\alpha}$, $\alpha = 0.5 - 1$) dominated regions are shown as the olive dotted lines. The optimum averaging time is defined as the time when the Allan variance shifts from the white noise dominated region to a drift dominated region; and lower panel: frequency distribution of the zero air mixing ratio for NO_2 (c) and CHOCHO (f).

Detection precisions for CHOCHO by BBCES instruments and other methods are compared in Table 1. A similar comparison of NO_2 measurement performance is given in Ref [27] for cavity-based instruments. The state-of-the-art performances of CHOCHO detection were achieved by Thalman and Volkamer [19] in 2010 and by Min et al. [22] in 2016. The reported 3σ detection precisions were 0.03 ppbv (60 s) with an L_{eff} of 13 km and 0.045 ppbv (5 s) with an L_{eff} of 17.8 km, respectively. The achievable sensitivity of BBCES depends on the number of photons injected into the cavity (which depends on the source brightness and beam imaging efficiency), L_{eff} (which depends on the cavity mirror quality and mirror separation), and how efficiently the various noise components are suppressed [27,51]. In this work, the light injection efficiency was improved with the cage-based configuration. The integration time of the CCD spectrometer in this work (20 ms) was over 7 times shorter than our previously reported aerosol extinction spectrometer [26] and a chemical amplification peroxy radicals measurement instrument [27], where a 150 ms integration time was needed to achieve the same level of transmission intensity. This design produces comparable detection precision (0.084 ppbv in 60 s) for CHOCHO to those of other CHOCHO instruments despite our instrument's much shorter L_{eff} (2.26 km). An important benefit of this configuration is that instrument can be more compact – this is desirable for producing a simple, robust, and stable analytical tool for field applications and mobile platforms. The detection sensitivity of our cage system could be further improved with cavity mirrors of higher reflectivity.

As the inlet losses of CHOCHO and NO_2 are assumed to be negligible [22], the accuracy of trace gas quantification by BBCES is mainly determined by the uncertainty in the literature reference cross sections and by the Rayleigh scattering cross sections used to calibrate the mirror reflectivity. The reported uncertainties in absorption cross sections are 3% for

Optics EXPRESS

CHOCHO and 1.1% for NO_2 [15]. The uncertainties in Rayleigh scattering cross sections are 4% for CO_2 and 1% for N_2 [39–41]. The total uncertainties (summed in quadrature) of the CHOCHO and NO_2 measurements were estimated to be about 5% and 4%, respectively.

Table 1. Comparison of CHOCHO detection precisions of BBCES instruments and other methods.

Analytical technique	Detection precision (ppbv, 3σ)	Sampling time	Year	Reference
Microfluidic GC	0.08 [a]	30 min [b]	2014	4
FTIR	2.5 [a]	5 min [c]	2014	4
LIP	0.011	5 min [c]	2008	6
DOAS	0.15 [a]	2-15 min [c]	2005	8
BBCES	0.09 [a] (d = 94.4 cm, L_{eff} = 17.9 km)	1 min [c]	2008	18
	0.03 [a] (d = 99 cm, L_{eff} = 13 km)	1 min [c]	2010	19
	0.07 [a,d]	20 s [c]	2014	4
	0.045 (d = 48 cm, L_{eff} = 17.8 km)	5 s [c]	2016	22
	0.084 (d = 42 cm, L_{eff} = 2.26 km)	**1 min [c, f]**	**2017**	**This work**
	0.024 [e]	**21 s [c, f]**		

[a] Adapted from Ref. [4]. [b] Offline techniques. [c] Online techniques. [d] The cavity length and effective absorption pathlength were not reported. [e] With application of real-time Kalman adaptive filtering. [f] The sampling time can be shortened by a factor of two without changing the data acquisition parameters.

3.3 Ambient measurement

Ambient measurement of CHOCHO and NO_2 was carried out at a suburban site over the period 1 to 3 August 2017. The instrument was located on the seventh floor of a building at the Anhui Institute of Optics and Fine Mechanics (31°54′18”N, 117°9′42”E) [24]. The site, which is on a peninsula and surrounded by water on three sides, is about 15 km west of the downtown center of Hefei city. Metropolitan Hefei has a population of 5.0 million. The instrument was installed in a temperature-controlled room maintained at 25 °C with a sample inlet about 1.5 m above the roof.

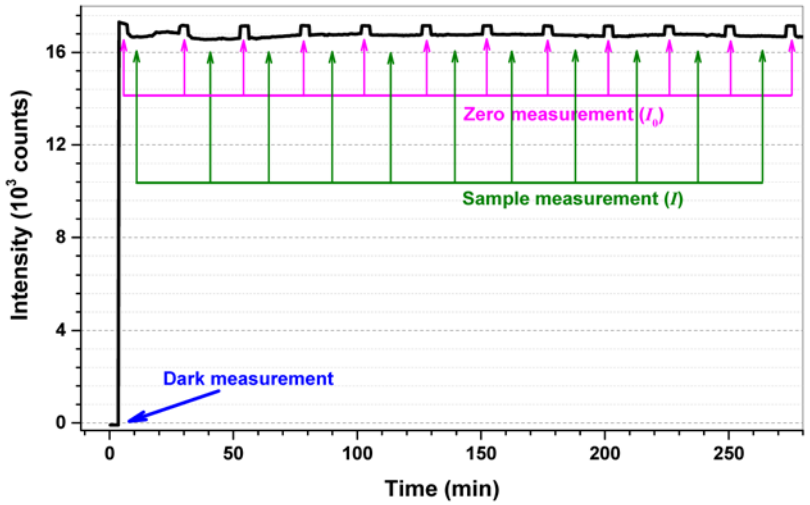


Fig. 5. Example time series of the transmitted intensity for each measurement at 460 nm.

Ambient air was directly sampled through a FEP tube (6 m long with an inner diameter of 1 cm) at a flow rate of 20 L min^{-1}. A fraction of the sample (1.5 L min^{-1}) was used for the BBCES measurement. The total acquisition time for each measurement was 21 s (for 20 ms integration time and 500 spectra averaging, and a 1 s data processing time). At the beginning of each measurement, the LED was switched off and the dark spectrum of the CCD spectrometer was recorded for later subtraction from the sample spectra. The cavity was

Optics EXPRESS

flushed with dry zero air every 20 min and the $I_0(\lambda)$ spectrum was acquired. An example time series of the transmitted intensity for single data pixels at 460 nm is shown in Fig. 5. With a 20 ms integration time, the dark intensity was about –92 counts, which contributed about 0.5% to the cavity transmission (~17200 counts). The ~0.1% I_0 intensity fluctuation within a single zero measurement indicated the high stability of the instrument; successive zero measurements had I_0 intensity changes of less than 100 counts, which were negligible contributions to the measurement uncertainty.

A typical BBCES spectrum and the data retrieval of ambient air with 8.64 ppbv NO_2 and 0.248 ppbv CHOCHO is shown in Fig. 6. A fit window of 445 – 465 nm was chosen to minimize the contribution of H_2O absorption. Under typical ambient relative humidity (RH) conditions, the contribution of H_2O absorption at 445 nm was about 10^{-9} cm^{-1}, a negligible contribution to the total absorption. The corresponding spectral fit residual is shown in the lower panel. A 1σ detection sensitivity of 7.5×10^{-10} cm^{-1} was achieved under these conditions. A time series of ambient CHOCHO and NO_2 measurement is shown in Fig. 6. An intercomparison of NO_2 measurements against alternative methods is not part of this study, but we note that our earlier broadband spectroscopy instruments have performed very well compared to commercial chemiluminescence detectors (Thermo 42i NOx analyzer) [24,28].

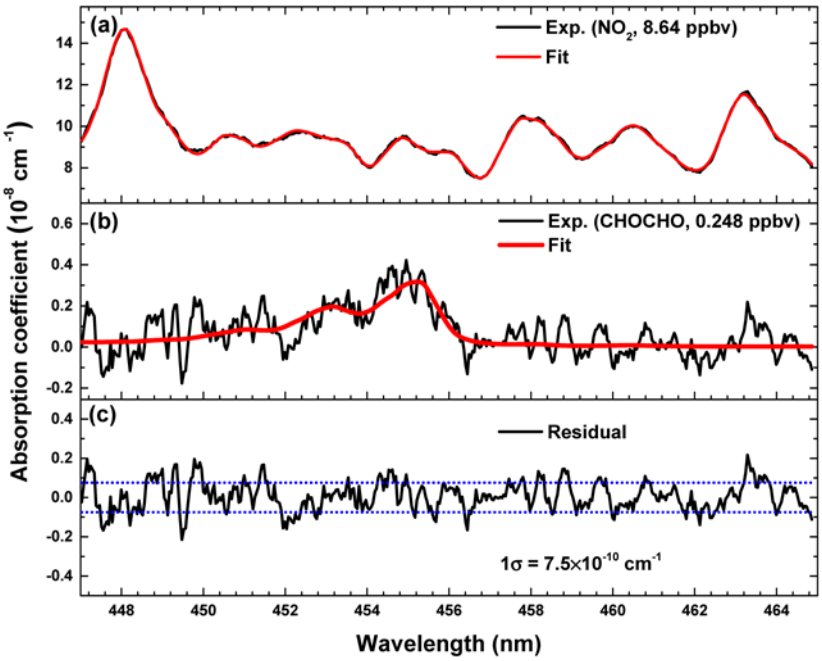


Fig. 6. Simultaneous measurement of ambient NO_2 (a) and CHOCHO (b) and the associated fit residual (c). The 1σ standard deviation of the fit residual was 7.5×10^{-10} cm^{-1} with 21 s total acquisition time for each spectrum.

3.4 Application of Kalman filtering to retrieved concentrations

To further improve the detection sensitivity and precision of the measured data, Kalman adaptive filtering [31,32,35] was applied in this work. As described in Refs [31] and [32], the 'true value' of the measurement at time k ($\hat{\delta}_k$) can be predicted from the combination of the measured value at time k (z_k) and the previously determined 'true value' at time k-1 ($\hat{\delta}_k^-$) by using a recursive procedure, as expressed by following equation:

Optics EXPRESS

$$\hat{\delta}_k = \hat{\delta}_k^- + K_k\left(z_k - \hat{\delta}_k^-\right) \tag{4}$$

The value of K_k is defined as the Kalman gain, and is related to the measurement noise introduced by the instrument (σ_v) and the true concentration variability (σ_w). The ratio of σ_v^2/σ_w^2, defined as ρ, is a constant value used to tune the filter. For small ρ values, the filtering is less efficient in removing shot-to-shot variation; where ρ is too large, the filtered result will lag behind true changes in concentration [32].

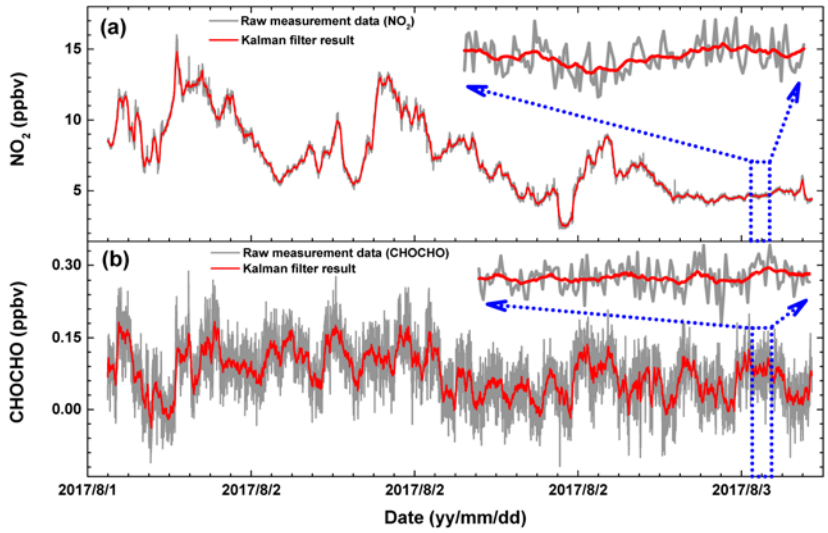


Fig. 7. Ambient air measurement of NO_2 (a) and CHOCHO (b) with the new BBCES instrument. A Kalman filter was used to improve the detection precision (red lines). The insets show a typical 1-h expanded view of the data with ρ set to 100.

The Kalman filter incorporates all available measurements, regardless of the precision of the initial values. In this work, the standard deviation of the first 20 measurement was used as the input of σ_v. The value of ρ was firstly set to 50, and was then adjusted to capture the sharp changes in the ambient NO_2 concentrations. Finally, a ρ value of 100 was chosen for the current system as one that provided a good compromise between improved precision and adequate time response. The red lines in Fig. 7 show the Kalman filtering results and clearly follow the true concentration changes. 1-h data without an obvious concentration change was used to evaluate the performance of Kalman filtering (as shown in the inserts of Fig. 7). When Kalman filtering was not used, the values of the concentration variability with 21 s total acquisition time were 0.09 and 0.033 ppbv for NO_2 and CHOCHO, respectively. With Kalman filtering, these values were reduced to 0.04 and 0.008 ppbv. The detection precisions were improved by a factor of 2 for NO_2 and by a factor of 4 for CHOCHO. Kalman adaptive filtering technique can efficiently reduce the real-time noise and shot-to-shot variability of concentration measurements without affecting the time resolution, and is demonstrated to be an effective tool for improving the quality of our real-time measurements.

4. Conclusion

In this paper, we report the development of a custom cage-based BBCES instrument for sensitive, real time *in situ* measurement of ambient CHOCHO and NO_2. With 60 s sampling time, 1σ detection precisions of 28 and 50 pptv for CHOCHO and NO_2 were achieved with an effective absorption pathlength of 2.26 km. Even better system performance could be achieved with mirrors of higher reflectivity, assuming that such mirrors do not make the instrument photon noise limited.

Optics EXPRESS

The cage system and the symmetrical interchangeability between transmitter and receiver units are advantageous: the configuration made the instrument more stable, compact, and easy to align, which improved the injection efficiency of light into the cavity. The fiber connectors also made the current instrument suitable for application to open-path measurement of trace gases [52] and aerosol [53]. The open-path configuration, while relatively unusual, is advantageous for monitoring target species that are susceptible to inlet losses, and for measuring aerosol extinction at ambient relative humidity, which would change rapidly if the ambient air temperature differed slightly from that of the instrument.

In this work, $I_0(\lambda)$ was obtained in particle-free zero air. If N_2 or He is used to get the reference spectrum and the spectral fit window is extended to 490 nm, the absorption of O_4 can also be used to determine the mirror reflectivity, essentially making BBCES an calibration-free method for trace detection [19,22,49,50].

The Kalman adaptive filtering technique was applied to the real-time simultaneous measurement of multiple species. Detection precisions were improved by a factor of 2 and 4 for field measurement of NO_2 and CHOCHO. The achievable precision, 24 pptv (3σ, 21 s) for CHOCHO measurement, was close to the state-of-the-art performance, but with a 6-8 times shorter effective absorption pathlength in this work. The performance evaluation demonstrated the potential applicability of Kalman filtering in the widely used BBCES technique.

Funding

National Key Research and Development Program of China (2016YFC0202205); National Natural Science Foundation of China (41375127); Natural Science Foundation of Anhui Province (1508085J03); the Youth Innovation Promotion Association CAS (2016383); and the China Special Fund for Meteorological Research in the Public Interest (GYHY201406039).

143.239.102.117 {ts '2018-09-25 07:22:00'}